**Academic year**
2023 - 2024

# 3D Surface Reconstruction from Optical Flat Measurements

**Ahmad Shakleya**

Bachelor's thesis
**Bachelor of Science in de industriële wetenschappen: elektronica-ICT**

Supervisor
**prof. dr. ing. J. Steckel, Cosys, UAntwerpen**

Cosupervisor
**ing. A. Aerts, Service Group Materials, UAntwerpen**

University of Antwerp
Faculty of Applied Engineering

# Contents

# 1. Preamble

# 2. Abstract

This thesis investigates the simulation and application of optical flats, essential in precision measurement science. It begins by detailing the challenges in simulating optical flats using ray-tracing in C++ and progresses to a successful Python-based approach that accurately models light interactions through intersecting planes. Results highlight that while ray-tracing effectively illustrates material and surface interactions, wavefront simulations provide clearer insights into light propagation and interference. The study confirms the utility of Python simulations in educational and research contexts, demonstrating their effectiveness in analyzing optical flat measurements. This work enhances the understanding of optical flats' properties and improves their practical applications.

# 3. Research Questions

This chapter outlines several key research questions that guide our investigation into the properties, simulation, and applications of optical flats. We begin by exploring the fundamental nature and characteristics of optical flats. This includes examining their material composition, surface quality, and the precision standards they meet in optical testing and engineering applications. Key aspects include the physical characteristics of optical flats, their operational principles, and the ongoing research in this area.

**How can we simulate an optical flat?** Our investigation next turns to the simulation of optical flats, focusing on creating virtual models that can predict and visualize the behavior of light when interacting with these surfaces. We discuss the potential of using a ray-tracing approach or a plane wavefront model, and weigh the advantages and disadvantages of each simulation method.

**How can we extract 3D surface shape from the measurements?** Another critical aspect of our research is extracting three-dimensional (3D) information from the interference patterns generated by optical flats. We review various methods from the literature for interpreting these fringe patterns and converting them into quantifiable 3D surface data, considering the integration of these methods with images generated from our simulations.

**Are the simulation and reconstruction representative enough?** Finally, we assess the representativeness of our simulations and reconstructions in various applications, examining how much the reconstructions deviate from the real models and exploring ways to enhance these reconstructions for better accuracy and practical utility.

# 4. Introduction

Optical flats are precision devices used in the field of material science to measure the flatness of surfaces or to create precisely flat surfaces. An optical flat is typically a high-quality, polished, flat glass or quartz disc used in conjunction with monochromatic light to form interference fringes that can be observed and measured to assess surface flatness or quality.Optical flats should be handled with great precaution as they are very fragile. [2, 3, 4, 5, 6]

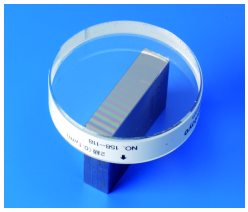

**Figure 4.1.:** Example of an optical flat. Figure taken from [1].

## 4.1. Physical Characteristics

### 4.1.1. Material Composition

Optical flats are predominantly made from two types of materials: fused silica and ultra-low expansion (ULE) glass. Fused silica, known for its exceptional optical clarity and thermal stability, is ideal for precision measurement tools. It has a very low coefficient of thermal expansion, which means it remains stable under varying temperatures, thereby minimizing measurement errors due to thermal variations (figure 4.2). [7]

Ultra-low expansion glass, such as Corning's ULE glass, is another favored material. This glass type is engineered to have extremely low thermal expansion rates, which are crucial in maintaining the accuracy of measurements in environments with fluctuating temperatures. ULE glass's robustness and resistance to thermal stress make it particularly suitable for high-precision optical applications, including astronomy and semiconductor manufacturing. [8]

Both materials are chosen not only for their minimal thermal properties but also for their ability to be polished to high optical qualities, ensuring that the optical flat does not introduce aberrations or distortions in the interference patterns used for surface measurements. [8, 7, 9]

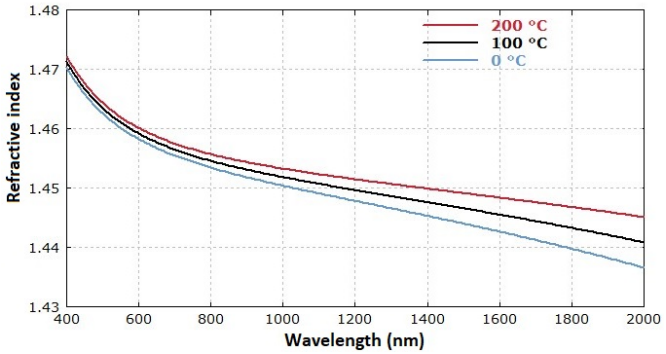


**Figure 4.2.:** The refractive index of fused silica versus wavelength at three different temperatures. Figure taken from [7].

### 4.1.2. Surface Quality

The surface of an optical flat is meticulously polished to achieve a high degree of flatness, typically within fractions of a wavelength of light ($\lambda/20$ or better). This extreme flatness is crucial for the accuracy of optical measurements. Any imperfections on the surface can distort the interference fringes, leading directly to measurement errors. [10]

After the initial polishing phases, optical flats may undergo additional processing steps such as the application of dielectric coatings. These enhancements are critical when the optical flats are used as reference mirrors in precision instruments like the Twyman–Green interferometer, where the utmost flatness is crucial. [6]

The final quality of optical flats is often verified in an interferometric setup, where they are compared against a reference surface that is of even higher precision. Occasionally, these reference surfaces may utilize fluids like mercury to achieve near-perfect flatness levels, although such materials are challenging to handle and maintain. [6]

## 4.2. Working Principle

The principle behind optical flats relies on the optical phenomenon of interference. This section delves into how interference fringes are formed, their types, and their importance in measuring surface characteristics.

### 4.2.1. Interference Fringes

Interference fringes are the result of the wave nature of light. When monochromatic light—light of a single wavelength—is used to illuminate the interface between an optical flat and another surface, variations in the gap created by surface irregularities cause the waves of light to overlap and interfere with each other. This interference can constructively or destructively affect the light waves, resulting in a pattern of dark and light bands known as interference fringes, which can be observed and analyzed.

#### 4.2.1.1. Formation of Fringes

Consider a setup where an optical flat is placed upon a surface to be tested under a monochromatic light source (figure 4.3). The light waves reflect off both the bottom surface of the optical flat and the top surface of the test object. Due to differences in the path traveled by the light waves—owing to variations in the gap between the two surfaces—these waves will interfere when they recombine. The condition for constructive and destructive interference is given by the equations:

$$2d\cos(\theta) = m\lambda, \quad \text{(constructive interference)} \qquad (4.1)$$

$$2d\cos(\theta) = (m+\frac{1}{2})\lambda, \quad \text{(destructive interference)} \qquad (4.2)$$

where:

- $d$ is the gap distance between the optical flat and the test surface,
- $\theta$ is the angle of incidence of the light,
- $m$ is an integer representing the order of the fringe,
- $\lambda$ is the wavelength of the light used.

When we dive in deeper on the waves we can see the following: constructive interference occurs when the path difference between the two waves is an integer multiple of the wavelength. Superposition of the waves result in bright fringes. [10]

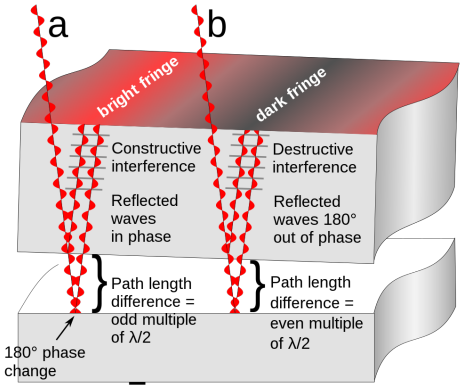


**Figure 4.3.:** Interference patterns due to light waves reflecting off an optical flat. On the left, bright fringes represent "Constructive interference" where reflected waves are in phase, caused by an odd multiple of half the wavelength ($\lambda/2$), amplifying the light intensity. On the right, dark fringes indicate "Destructive interference" with waves 180 degrees out of phase due to an even multiple of $\lambda/2$, canceling out the light. A key feature is the 180-degree phase change at the boundary, crucial for the formation of these patterns. Figure taken from [10].

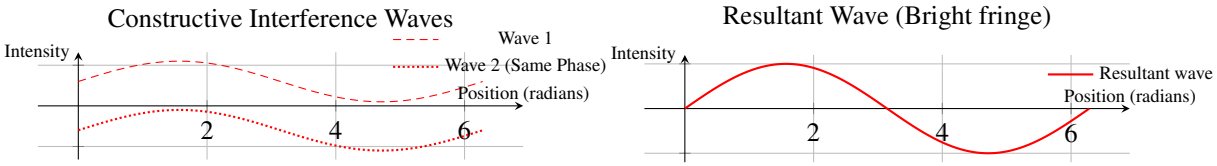


**Figure 4.4.:** 2 lightwaves with the same phase resulting in a bright fringe.

Destructive interference, on the other hand, occurs when the path difference is a half-integer multiple of the wavelength, resulting in dark fringes. [10]

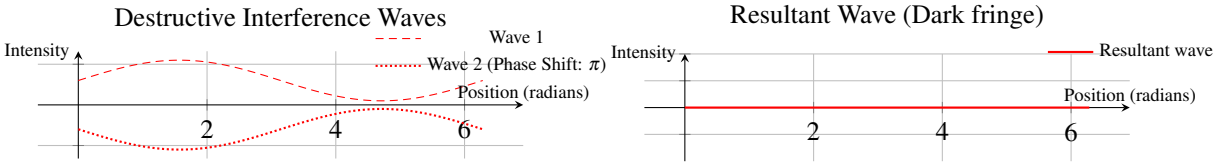


**Figure 4.5.:** 2 lightwaves out of phase resulting in a dark fringe.

#### 4.2.1.2. Analysis of Fringe Patterns

The pattern of the fringes provides information about the surface's properties:

- **Straight and Parallel Fringes** indicate that the test surface is precisely flat. In this scenario, the fringes are parallel and uniformly spaced.
- **Curved Fringes** suggest that the surface is convex or concave. The curvature of the fringes gives clues about the curvature of the surface itself.
- **Irregular Fringes** are indicative of surface defects, bumps, or dips. The irregularity in spacing or the fringe shape can be analyzed to quantify the nature of the surface flaws.

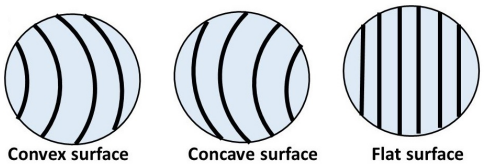


**Figure 4.6.:** Different types of interference fringe patterns and what they indicate about surface characteristics. Figure taken from [11].

## 4.3. Innovations in Optical Flat Technology

### 4.3.1. Plasmonic Optical Flat

Recent advancements have expanded the traditional concept of optical flats to include plasmonic optical flats, which utilize nanostructured plasmonic surfaces. This innovation stems from the field of plasmonics, where the manipulation of light at the nanoscale allows for extreme localization and sensitivity to environmental changes. Plasmonic optical flats, comprised of nanostructured metal arrays, significantly enhance the sensitivity and resolution of surface inspections beyond the diffraction limit of light. These new optical flats are particularly effective in detecting sub-wavelength surface anomalies and offer the potential for rapid and precise surface inspection using simple, low-cost equipment. [12]

### 4.3.2. Phase Measuring Deflectometry

A novel approach in the measurement of optical flats involves Phase Measuring Deflectometry (PMD), which offers a flexible and cost-effective alternative to interferometry. PMD uses a triangulation method involving a pinhole camera and LCD display to generate sinusoidal fringes, which are reflected by the flat surface. Distortions in these fringes are then captured and analyzed to determine the surface's figure. This technique is particularly advantageous for measuring surfaces where high slopes at edges or environmental sensitivities present challenges to traditional methods. The integration of PMD into optical flat metrology represents a significant shift towards more dynamic and accessible measurement technologies. [13]

## 4.4. Fringe Analysis in Optical Metrology

Fringe analysis is an indispensable technique in the field of optical metrology, providing a non-intrusive means to capture and quantify physical phenomena with high precision. This method leverages the wave nature of light to generate fringe patterns, which are essentially contour maps representing variations in optical path length due to changes in physical properties like surface height, deformation, and refractive index changes.

The principle behind fringe analysis involves the interaction of light waves either through interference in interferometry or through projection in fringe projection techniques. In both instances, the resulting fringe patterns contain encoded information about the object's surface or the physical phenomenon being studied. The challenge, however, lies in converting these fringe patterns into quantitative data, a process that is achieved through various computational methods.

This chapter was mainly inspired by `Chapter 21: Fringe Analysis` in `Handbook of Optical Metrology by Toru Yoshizawa` [14]

### 4.4.1. Techniques in Fringe Analysis

Two primary approaches define the landscape of fringe analysis:

1. **Multiple-Input Image Techniques:** This approach utilizes multiple images of the fringe pattern, each obtained at a different phase shift. Common methods include the phase-shifting technique, where the phase of the reference beam is varied systematically to produce different fringe patterns, and the fringe scanning method, where the object or the fringe generator itself is moved to vary the fringe pattern.

2. **Single-Input Image Techniques:** In scenarios where dynamic measurements are required, or it is impractical to obtain multiple images, single-input image techniques are employed. The Fourier Transform method is the most notable, using a single image with carrier fringes to extract phase information through spatial frequency analysis. We will elaborate more on this in the following section.

### 4.4.2. Fourier Transform Method

The Fourier Transform (FT) method of fringe analysis represents a significant advancement in the field of optical metrology, particularly for dynamic measurements where the acquisition of multiple sequential images is impractical. This method, utilizing a single fringe image with carrier fringes, simplifies the setup and accelerates data processing, making it ideal for real-time applications.

#### 4.4.2.1. Principle of Operation

The FT method involves the acquisition of a single fringe pattern that includes high-frequency carrier fringes. These carrier fringes are typically introduced by slightly tilting a reference beam in an interferometer setup, resulting in a fringe pattern with a well-defined spatial frequency. The mathematical basis of this approach is to model the intensity distribution of the fringe pattern as a sum of sinusoidal functions whose amplitudes encode the phase information of the surface being analyzed.

$$I(x,y) = a(x,y) + b(x,y)\cos[2\pi f(x,y) + \phi(x,y)] \tag{4.3}$$

Here, $I(x,y)$ represents the recorded intensity, $a(x,y)$ is the background illumination, $b(x,y)$ denotes the amplitude of the modulation, $f(x,y)$ is the carrier frequency, and $\phi(x,y)$ is the phase to be recovered.

#### 4.4.2.2. Fourier Transform and Filtering

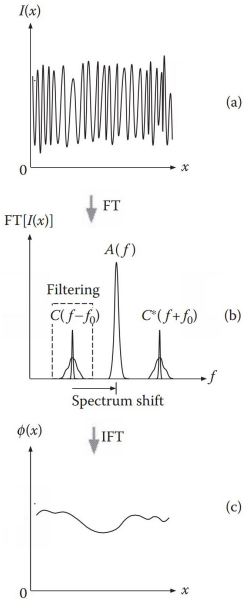


**Figure 4.7.:** 1D Signal processing flow in FT method. (a) Phase-modulated carrier fringes. (b) Filtering and shift in spectrum space. (c) Demodulated phase. This procedure can easily be extended to the 2D FT and filtering in a 2D frequency space. Figure taken from [14].

The core step in the FT method is the Fourier transform of the recorded intensity distribution, which separates the frequency components. The high spatial frequency of the carrier fringes ensures their separation from the lower spatial frequency background. By filtering and isolating the frequency component corresponding to the carrier fringes, the phase information embedded in the fringes can be extracted effectively.

$$\hat{I}(f_x, f_y) = \mathscr{F}\{I(x,y)\} \tag{4.4}$$

Here, $\hat{I}(f_x, f_y)$ represents the 2D Fourier transform of the intensity distribution. Filtering around the carrier frequency $f_0$ isolates the relevant phase information.

#### 4.4.2.3. Phase Demodulation and Reconstruction

After filtering, the isolated component is shifted to zero frequency, and an inverse Fourier transform is applied to reconstruct the phase-modulated image. The phase at each point of the image can then be calculated using the arctan function applied to the real and imaginary parts of the reconstructed image.

$$\phi(x,y) = \arctan\left(\frac{\mathrm{Im}[\mathscr{F}^{-1}(\hat{I}(f_x,f_y))]}{\mathrm{Re}[\mathscr{F}^{-1}(\hat{I}(f_x,f_y))]}\right) \tag{4.5}$$

This reconstructed phase map provides a direct measurement of the optical path differences induced by the object's surface, translating physical deformations into measurable phase shifts.

#### 4.4.2.4. Rationale for Using the Fourier Transform Method

The adoption of the Fourier Transform (FT) method in fringe analysis is driven by several practical and academic motivations, particularly suited to scenarios where obtaining multiple images with varied fringe patterns is challenging. One such scenario is when using an optical flat, which typically produces only one image. The inherent difficulty in capturing multiple images with different fringe patterns at the exact same position makes the FT method highly valuable. This method can extract detailed phase information from a single static image, circumventing the need for moving the setup to introduce different phase shifts, which is often impractical or impossible with an optical flat.
Additionally, my interest in applying signal processing techniques beyond theoretical mathematics classes has led me to explore the use of Fourier Transform in a practical, real-world application. The FT method offers a profound application of Fourier analysis, allowing the decomposition of an image into its frequency components. This not only aids in isolating the phase information crucial for metrological assessments but also reinforces the foundational signal processing principles by applying them to solve complex engineering problems.
Note that this method only works if the picture is taken perpendicular to the surface of the optical flat.

### 4.4.3. Phase Unwrapping

Phase unwrapping is an essential process in fringe analysis, addressing the intrinsic limitation where phase measurements are typically confined within a $[-\pi, \pi]$ interval, known as phase wrapping. This phenomenon occurs because the phase response of the imaging system is cyclic, with each cycle representing a change in phase of $2\pi$. Hence, any phase change beyond this range results in a modulo $2\pi$ calculation, which can obscure the true phase changes caused by the physical properties of the object being studied.

#### 4.4.3.1. Challenges of Phase Wrapping

In practical applications, such as 3D surface profiling or deformation analysis, this wrapping effect can create discontinuities in the computed phase map, appearing as abrupt jumps from $-\pi$ to $\pi$ and vice versa. These discontinuities can significantly distort the resulting measurements, making it impossible to directly infer the true topographical features of the surface under investigation without additional processing.

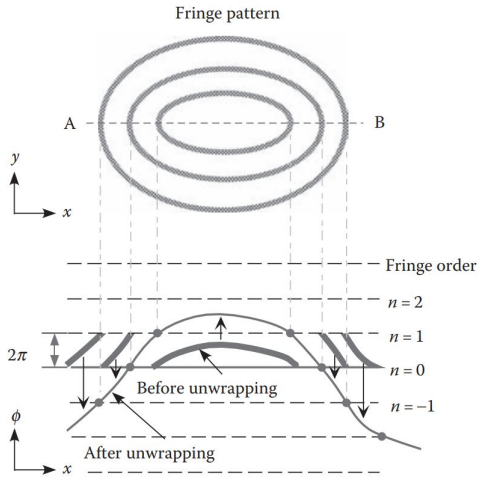


**Figure 4.8.:** Phase unwrapping: a fringe pattern above and a phase unwrapping diagram below. The fringe pattern consists of concentric circles representing equal phase levels, highlighted by specific points $A$ and $B$, and intersected by lines indicating fringe orders $n = -1, 0, 1, 2$. Below, the phase $\phi$ along the $x$-axis is initially depicted with jumps of $2\pi$, typical in raw data from interferometric measurements. The phase unwrapping section smooths these jumps to create a continuous line, providing a clearer, more accurate representation of phase variations. Figure taken from [14].

#### 4.4.3.2. Unwrapping Algorithms

Phase unwrapping seeks to mitigate these issues by reconstructing the original phase distribution that extends beyond the $[-\pi, \pi]$ range. The process involves algorithmically adding or subtracting $2\pi$ where necessary to eliminate the discontinuities, thereby 'unwrapping' the phase to reflect the true surface characteristics.

#### 4.4.3.3. Simple Phase Unwrapping Using Adjacent Pixel Comparison

In the most straightforward cases of phase unwrapping, the goal is to correct phase discontinuities along a specified path, typically one-dimensional, across the image. This method involves comparing the phase values of adjacent pixels and making corrections when abrupt changes are detected that indicate wrapping. The process is governed by the following set of rules:

$$\phi_{\text{unwrapped}}(i) = \begin{cases} \phi(i) - 2\pi & \text{if } \phi(i) - \phi(i-1) > \pi \\ \phi(i) + 2\pi & \text{if } \phi(i) - \phi(i-1) < -\pi \\ \phi(i) & \text{otherwise} \end{cases} \tag{4.6}$$

where $\phi(i)$ is the wrapped phase at pixel $i$ and $\phi_{\text{unwrapped}}(i)$ is the corrected phase value. This method assumes a sequential progression through the image pixels, typically from left to right or top to bottom.

Phase unwrapping can be particularly challenging in scenarios where fringe patterns are surrounded by nonrectangular boundaries or contain singular points—locations where the fringe modulation is very low or the phase differences exceed $2\pi$. In such cases, the phase unwrapping path may be accidentally interrupted, leading to deviations from the true phase distribution. To address these complexities, several robust algorithms have been developed:

- **Minimum-Spanning Tree (MST) Algorithms:** These methods create a continuous phase-unwrapping path by spanning the effective phase area with tree-like trajectories. They are designed to avoid creating localized loops and use cost functions such as the spatial phase gradient and fringe contrast to assess and ensure the reliability of the pixels. Unreliable pixels are identified and removed from the spanning tree, facilitating a smoother unwrapping process.
- **Energy Minimization Algorithms:** This approach involves minimizing an energy function that quantifies the discontinuities in the phase map. The algorithm iteratively adjusts the phases by $\pm 2\pi$ to reduce the total energy, aiming for a state where the sum of squared differences of neighboring pixels is minimized. This method is particularly effective as it does not rely on a predefined path and can adapt to the local characteristics of the phase data.
- **Error Correction and Singular Point Handling:** Before unwrapping, it is crucial to identify and address singular points where errors are likely due to low modulation or high noise. Techniques include using local operations to assess the consistency of the phase differences around these points. If necessary, lines connecting points of opposite discontinuity signs are established as boundaries not to be crossed during the unwrapping process.

# 5. Methods and Materials

## 5.1. Initial Approach Using Ray Tracing in C++

**Ray tracing** is a rendering technique that simulates the way light interacts with objects to generate images with high visual realism. Unlike rasterization, which is used in most real-time graphics, ray tracing calculates the color of pixels by tracing the path that light would take as it travels through a scene. This path is traced backwards from the viewer's eye to the light source, a method known as *backward ray tracing*.

Initially, the simulation of optical flat measurements was attempted using a ray tracing technique in C++. Ray tracing is a powerful computational method for simulating the path of light through media. It models the propagation of light rays and their interactions with surfaces, which is particularly useful in optical studies where the understanding of light behavior in precise environments is necessary. However, this approach did not yield successful results due to complexities in accurately modeling the intricate interference patterns that are critical in optical flat evaluations.

## 5.2. Successful Simulation Using Python

After the initial setbacks, a more successful simulation was developed using Python. This method utilized the concept of intersecting planes with the surface under test (sft) (see figure 5.1). Each plane was separated by half the wavelength of the light transmitted through the optical flat, allowing for the simulation of interference patterns by modeling how these planes interact with the sft irregularities as can be seen in figure 5.2.

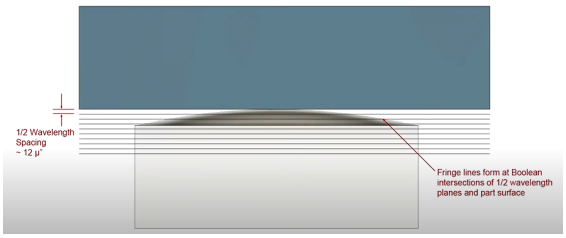


**Figure 5.1.:** The blue area at the top represents an optical flat placed over a test surface shown in grey. The white lines, spaced half a wavelength apart, are interference fringes. These fringes form at points where the height difference between the optical flat and the surface matches multiples of half the light's wavelength. The pattern of these fringes reveals the topography of the surface beneath the flat. Figure taken from [15].

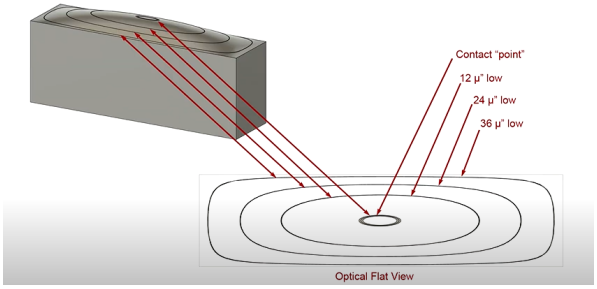


**Figure 5.2.:** A 3D model with an optical flat above a test surface and a 2D projection. Red lines represent light rays reflecting at different gaps between the optical flat and the surface. These variations are visible in the 2D "Optical Flat View" as concentric circular fringes, each indicating a constant air gap. This method precisely measures the deviations in surface flatness, with each ring in the diagram quantifying specific irregularities. Figure taken from [15].

### 5.2.1. Backend Development: Python Scripts

To implement this method, several Python scripts were created:

- **Intersection** - This function, as can be seen in figure 5.3, handles the mathematical computation of plane and surface intersections, critical for modeling how light interacts with different surfaces.
- **Disk, Cylinder, Flat_surface, Shape3D, STLFigure** - These classes contribute to generating and handling various geometrical shapes and rendering the final 3D images which represent the simulation results.

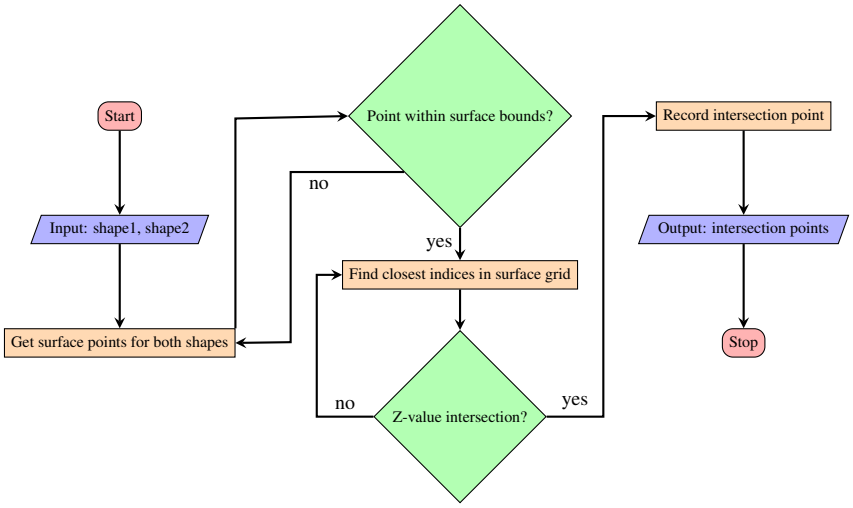


**Figure 5.3.:** Flowchart of the intersection function: initially, it extracts the $x$, $y$, and $z$ coordinates from both (`shape1`) and (`shape2`) using their `get_surface()` methods. Lists are then initialized to store the coordinates of the intersection points. The function determines the bounds of (`shape1`) and iterates over each (`shape2`) point, checking if it lies within these bounds. For each in-bound point, it identifies the closest surface points in the $x$ and $y$ dimensions. If a (`shape2's`) $z$-value matches closely with the $z$-value at these points, within a tolerance of $\pm 0.01$, the point is recorded as an intersection. The function ultimately returns these intersection points as NumPy arrays.

### 5.2.2. Frontend Development: Graphical User Interface (GUI)

A comprehensive GUI developed through `Gui.py` facilitates user interaction with the simulation, allowing for real-time adjustments and visualization of results. The GUI is structured into several functional tabs, each enhancing usability and educational value. Screenshots of the GUI can be found in the appendix.

#### 5.2.2.1. GUI Components Detailed Descriptions

**File Tab** This tab manages file operations such as importing and exporting configurations. Functions include:

- **Export Configuration** - Opens a file dialog to save configurations in JSON format. After selection, it executes the export shapes command and confirms the operation.
- **Import Configuration** - Similar to export, this function loads configurations from a JSON file, redraws shapes based on the new data, and confirms the import.

**Insert Tab** This tab facilitates the insertion of various 3D shapes into the simulation. Each subtab provides specialized controls for inserting and configuring objects such as cylinders, disks, flat surfaces, optical flats and STL figures.

**View Tab** This tab allows users to customize the visual aspects of the application: users can modify the text color, background color, and font.

**Help Tab** This tab includes a PDF viewer for accessing documentation directly within the GUI so users can effectively utilize the simulation tool without Internet connection.

**Log Tab** This tab records and displays logs of user actions and system responses.

**3D View Tab** This tab provides a dynamic 3D visualization space where users can interact with the models.

#### 5.2.2.2. 3D View Tab Detailed Description

The `ThreeDViewTab` class is the most important tab of the GUI, designed to provide interactive 3D visualizations of the simulated environment. This tab is important to assess the accuracy and spatial relationships of the models within the simulation. It integrates a Matplotlib 3D plot within the interface and renders graphical representation of the shapes.

##### Interaction and Visualization

- **Shape Manipulation Methods**: Includes adding new shapes, drawing updates on the Matplotlib canvas, and managing shape deletions — all reflected visually in real-time.
- **Interactive Features**: Allows users to interact with the 3D models via mouse and keyboard inputs to rotate, zoom, and pan across different views, providing a comprehensive understanding of the model's geometry and spatial properties.

##### Utility Functions

- **Update States**: Dynamically adjusts the state of GUI controls based on the context (e.g., whether shapes are present or a particular shape is selected).
- **Calculate Intersections**: Uses the intersection function as described above to determine and visualize intersections between different shapes.

#### 5.2.2.3. Reconstruction GUI Components

The `Help Tab` and the `Log Tab` have the same functionalities as above, so I won't discuss them here.

**Image Processing Tab** The `Image Processing Tab` class extends the capabilities of the graphical user interface by incorporating image processing techniques.

1. **Fourier Transforms:** This tab utilizes the Fourier transform, a mathematical technique that transforms spatial data into frequency data. This is crucial for identifying periodic structures in images, as well as for noise reduction and image enhancement.
2. **Frequency Filtering:** After transforming the image to the frequency domain, specific frequencies like the carrier frequency can be isolated or suppressed to enhance certain image features or remove unwanted artifacts. This process involves applying a mask to the Fourier transform of the image that selectively retains or removes certain frequencies.
3. **Phase Extraction:** This feature extracts the phase from the complex representation of the Fourier-transformed image. The phase of the image carries important structural information that is not visible in the amplitude alone. Extracting and analyzing the phase is essential to reconstruct three-dimensional shapes from two-dimensional images.
4. **Phase Unwrapping:** Phase images, by nature, are wrapped around a $2\pi$ interval which creates discontinuities that can complicate further analysis. Phase unwrapping corrects these discontinuities to produce a continuous phase map that accurately represents changes across the image.
5. **Height Map Calculation:** Utilizing the unwrapped phase, this function calculates height maps from phase images, where the optical path difference at each pixel translates to physical height variations. This is particularly useful in surface profilometry and interferometric microscopy.
6. **Height Map Smoothing:** The calculated height maps can often contain noise and other high-frequency components that obscure the true surface features. Smoothing, typically using Gaussian filters, helps to mitigate these effects, enhancing the visual quality and interpretability of the height maps.

7. **Visualization and Interaction:** Integration with `matplotlib` for visualizing results allows users to see the processed images in various forms, including 3D plots of height maps. This interactive visualization aids in the qualitative analysis of the data and provides a dynamic way to explore the impact of different processing parameters.

# 6. Results

## 6.1. Simulation of an Optical Flat

The evaluation of both ray-tracing and wavefront simulation models in the simulation of optical flats has demonstrated that the integration of these methods provides a clear depiction of optical behaviors. Ray-tracing accurately models the interactions of light waves with optical flats, reflecting the inherent properties of materials and nuances of surface quality. Altough the ray-tracing engine worked, this result was not achieved in this bachelorthesis. Complementary to this, wavefront simulations effectively visualized the propagation and interference of light waves as they interact with surfaces.

### 6.1.1. Simulation Results

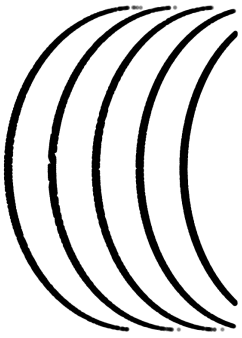

**Figure 6.1.:** Simulated interference pattern generated by the application. The red dot depicts the place of the hinge of the optical flat. More fringes and more continuity in the fringes can be achieved by adjusting the `num_disks` and the `resolution` parameters.

The simulation functionalities within the application were tested to analyze their performance in replicating realistic scenarios. Through the use of the Python-based simulation modules, we were able to perform intersection and visualize interference patterns. Figure 6.1 shows a typical simulation output, illustrating the precision and clarity achieved.

## 6.2. Extraction of 3D Surface Shape from Measurements

Employing the Fourier Transform (FT) method to extract 3D shapes from optical measurements was the key factor to achieve this result. This technique captures fringe patterns embedded with high-frequency carrier fringes and applies Fourier transform techniques to isolate these fringes and recover detailed phase information. The efficacy of this approach is showcased by its ability to convert interference patterns into quantifiable 3D surface maps.
The integration of phase unwrapping and height map calculation features within the GUI simplifies data processing and reduces the time required for analysis. This functionality facilitates the direct transformation of phase data into 3D topographical maps.

### 6.2.1. Surface Topography Visualization

The GUI's 3D view tab provides an interactive visualization of reconstructed surfaces. We could manipulate the view to better understand the topographical details of the surface being studied. An example of a reconstructed surface is shown in Figure 6.2.

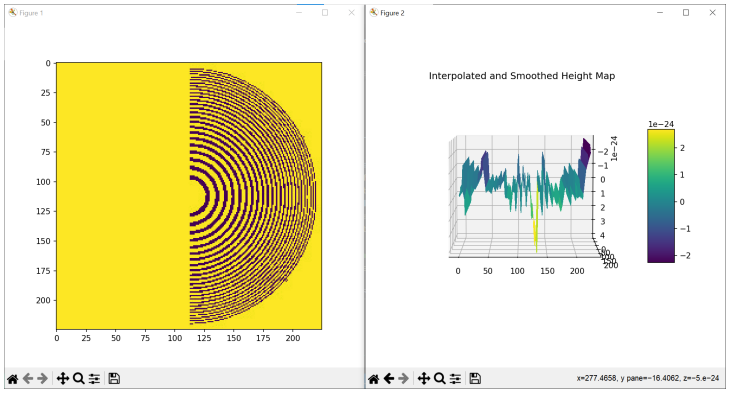


**Figure 6.2.:** 3D visualization of surface topography as reconstructed by the application.

## 6.3. User Interaction and GUI Performance

The modular design of the GUI proved to be highly effective in facilitating user interaction with datasets and processing tools. The application's responsiveness and stability during high-computation tasks were also good.

## 6.4. Representativeness of Simulation and Reconstruction

The representativeness of the simulations and reconstructions was not evaluated due to lack of time.

# 7. Discussion

## 7.1. Research Goals

As highlighted in the introduction, the primary objective of this research was to develop a robust simulation and reconstruction tool capable of accurately modeling and analyzing optical flat measurements. The simulation results demonstrated that the Python-based modules could successfully replicate realistic optical interactions and interference patterns. This aligns well with the project's aim, as stated in our initial research questions.

The method of using planes separated by specific intervals corresponding to the light wavelength proved effective in simulating the necessary conditions to study optical flats. The Python environment, complemented by a user-friendly GUI, enhanced the flexibility and accessibility of the simulation, making it a robust tool for both educational and research applications in optical measurements.

The ability to reconstruct accurate phase maps and 3D surface topographies from both simulated and real-world data underlines the effectiveness of the Fourier Transform methods and phase unwrapping techniques employed. These results directly correlate with the approaches discussed in the Methods and Materials section, where the integration of image processing algorithms was used to significantly improve the accuracy and reliability of optical flat measurement analysis.

## 7.2. Representativeness and Limitations of 3D Reconstruction

Despite the successes, the 3D reconstruction process was not fully representative in some aspects. This was partly due to the limits of the hardware used, which could not always capture the full depth and detail required for a fully representative fringe model unless it takes too long to compute.. This limitation is due to the hardware. Additionally, the software uses a binary representation for the interference fringes, in which there are sharp transitions between dark fringes and bright fringes. This causes the 3D representation to show sharp transistions.

Moreover, the lack of evaluation against known standards or real samples, as noted in the Results section, prevented a thorough validation of the representativeness of the reconstructed models. This evaluation should indicate that the methods are designed to minimize errors of the simulations and reconstructions. Iterative testing and refining of the simulation parameters should show that they closely align with actual measurements.

## 7.3. Future Directions

To address these limitations, future research could focus on integrating multi-modal imaging techniques that combine optical measurements with other forms of data acquisition, such as a deflectometer or a CMM, to enhance the depth and accuracy of the 3D reconstructions. Also, more interference fringes could be simulated using not only intersections with planes at half the wavelength used, but also the in between values.

## 7.4. Conclusion

The application successfully demonstrated its capability in both simulating and reconstructing optical flat measurements, supported by a user-friendly and powerful graphical interface. Future work will focus on expanding the range of simulations.

Although we initially lost a lot of time developing a ray-tracing engine to incorporate light interference phenomena, we did not succeed. We have found a solution that is very close to reality and very versatile. With STL file support, any optical flat measurement can be modeled, provided the STL file of the surface under test is available.

# Bibliography


[1] Mitutoyo UK, "Optical flat – mitutoyo," 2023, accessed: 2024-05-11. [Online]. Available: https://shop.mitutoyo.co.uk/web/mitutoyo/en_GB/mitutoyo/$catalogue/mitutoyoData/PR/158-118/datasheet.xhtml 3

[2] Y. Toru, *Handbook of Optical Metrology: Principles and applications*. CRC Press, 2017. [Online]. Available: https://www.taylorfrancis.com/books/edit/10.1201/b18328/handbook-optical-metrology-toru-yoshizawa 3

[3] Edmund Optics, "Optical flats," 2024, accessed: 2024-05-11. [Online]. Available: https://www.edmundoptics.com/knowledge-center/application-notes/optics/optical-flats/ 3

[4] Kemet, "Optical flats," 2024, accessed: 2024-05-11. [Online]. Available: https://www.kemet.co.uk/products/flatlapping/optical-flats 3

[5] Lapmaster Wolters, "Optical flats," 2024, accessed: 2024-05-11. [Online]. Available: https://www.lapmaster-wolters.com/optical-flats.html 3

[6] R. Paschotta, "Optical flats," RP Photonics Encyclopedia, available online at https://www.rp-photonics.com/optical_flats.html. [Online]. Available: https://www.rp-photonics.com/optical_flats.html 3

[7] ——, "Fused silica," RP Photonics Encyclopedia, Available online at https://www.rp-photonics.com/fused_silica.html. [Online]. Available: https://www.rp-photonics.com/fused_silica.html 3

[8] "Corning® ule® glass," Jul 2022. [Online]. Available: https://www.corning.com/worldwide/en/products/advanced-optics/product-materials/semiconductor-laser-optic-components/ultra-low-expansion-glass.html 3

[9] M. V. Mantravadi and D. Malacara, *Newton, Fizeau, and Haidinger Interferometers*. John Wiley & Sons, Ltd, 2007, pp. 1–45. [Online]. Available: https://onlinelibrary.wiley.com/doi/abs/10.1002/9780470135976.ch1 3

[10] W. contributors, "Optical flat — wikipedia, the free encyclopedia," https://en.wikipedia.org/w/index.php?title=Optical_flat&oldid=1212101911, 2024, accessed: 2024-05-11. 3, 4

[11] T. Joji, "Optical flat," Jun 2023, accessed: 2024-05-11. [Online]. Available: https://youtu.be/tmFurBsknPc?si=iAR_TBQgxoM2s4Gn 4

[12] Y. Zheng, J. Bian, X.-L. Wang, J.-X. Liu, P. Feng, H.-X. Ge, O. J. F. Martin, and W.-H. Zhang, "Revisiting newton's rings with a plasmonic optical flat for high-accuracy surface inspection," *LIGHT-SCIENCE & APPLICATIONS*, vol. 5, OCT 2016. 5

[13] E. Kewei, D. Li, L. Yang, G. Guo, M. Li, X. Wang, T. Zhang, and Z. Xiong, "Novel method for high accuracy figure measurement of optical flat," *OPTICS AND LASERS IN ENGINEERING*, vol. 88, pp. 162–166, JAN 2017. 5

[14] T. V. Yoshizawa and J.-i. Kato, *Fringe Analysis*. CRC Press, 2015, pp. 513–524. [Online]. Available: https://www.taylorfrancis.com/books/edit/10.1201/b18328/handbook-optical-metrology-toru-yoshizawa 5, 6

[15] Reading optical flats part 1. Youtube. [Online]. Available: https://www.youtube.com/watch?v=ebwEOueCBvE 8

# A. Appendix

## A.1. Screenshots of the GUI

### A.1.1. 3D Shape Configuration and Visualization

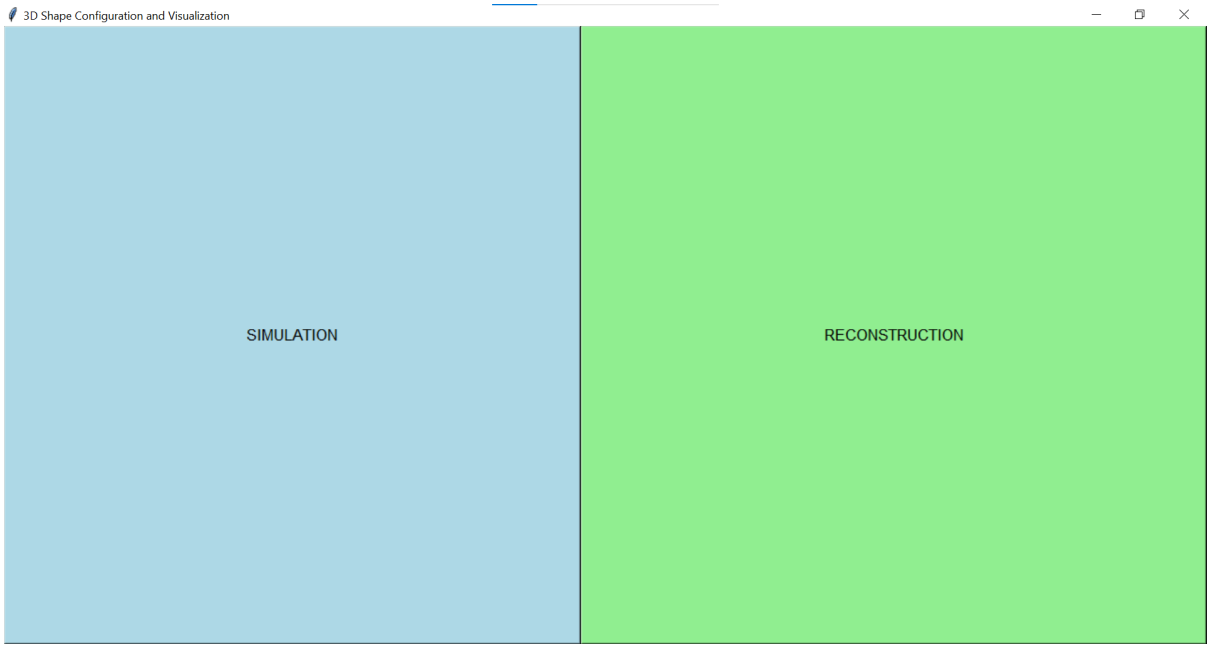


**Figure A.1.:** Initial interface showing two divided sections for simulation and reconstruction processes in the 3D Shape Configuration and Visualization tool.

### A.1.2. Simulation Window - Insert Cylinder

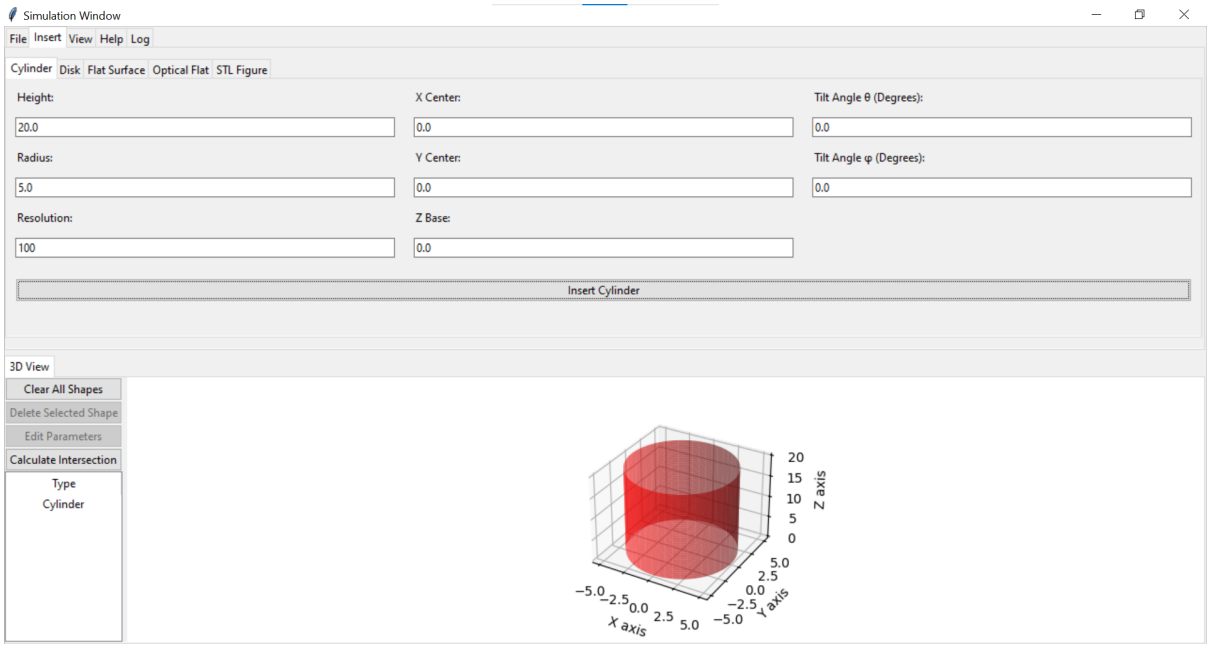


**Figure A.2.:** Simulation window displaying the parameters for inserting a cylinder and a 3D view of the inserted cylinder with default orientation.

### A.1.3. Cylinder and Optical Flat Intersection

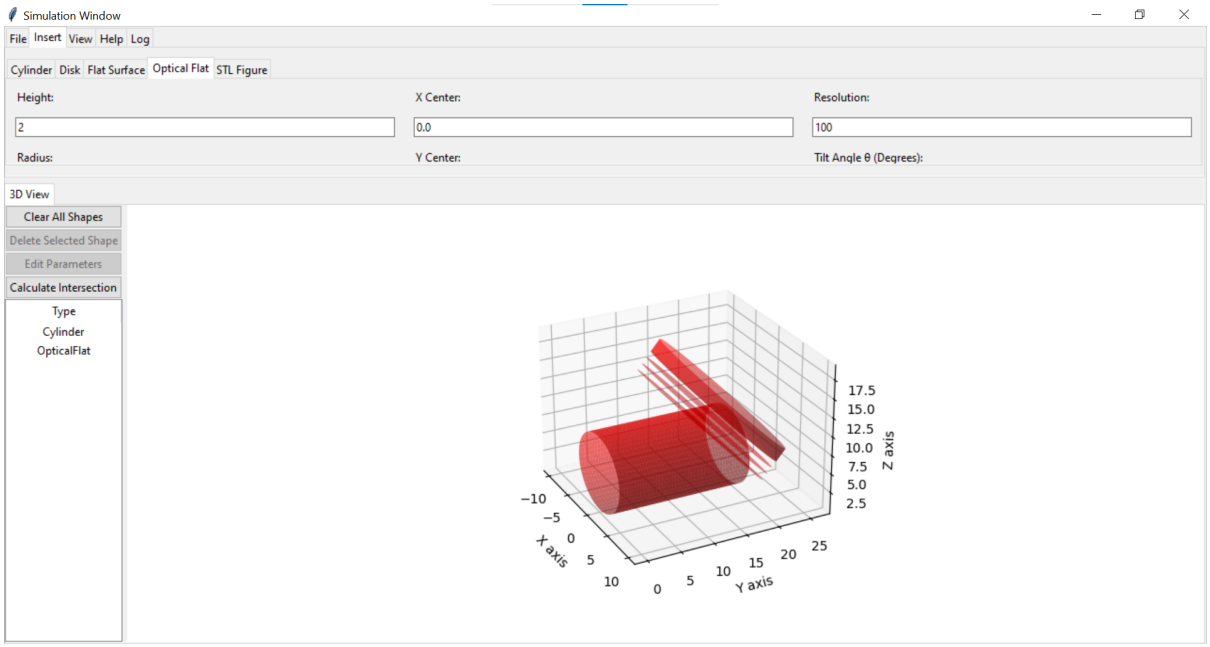


**Figure A.3.:** Demonstration of a cylinder intersecting with an optical flat at an angle, visualized in the simulation window.

### A.1.4. Updated Cylinder Position

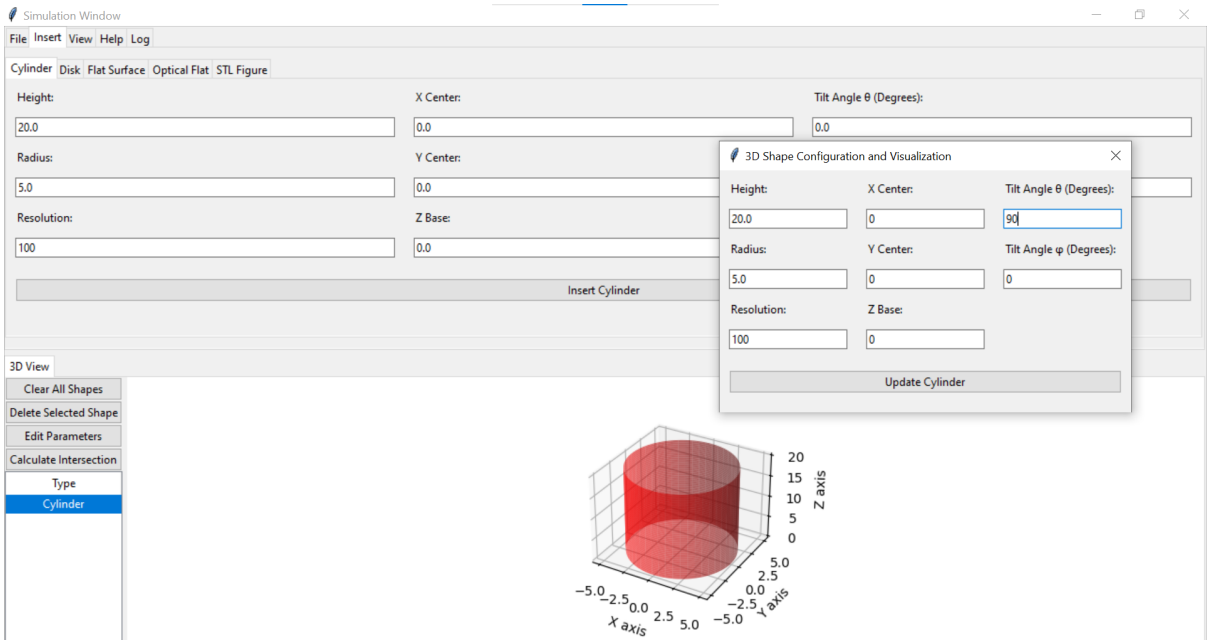


**Figure A.4.:** Updated visualization showing the cylinder rotated by 90 degrees about the Z-axis to illustrate manipulation capabilities.

### A.1.5. Optical Flat with Multiple Disks

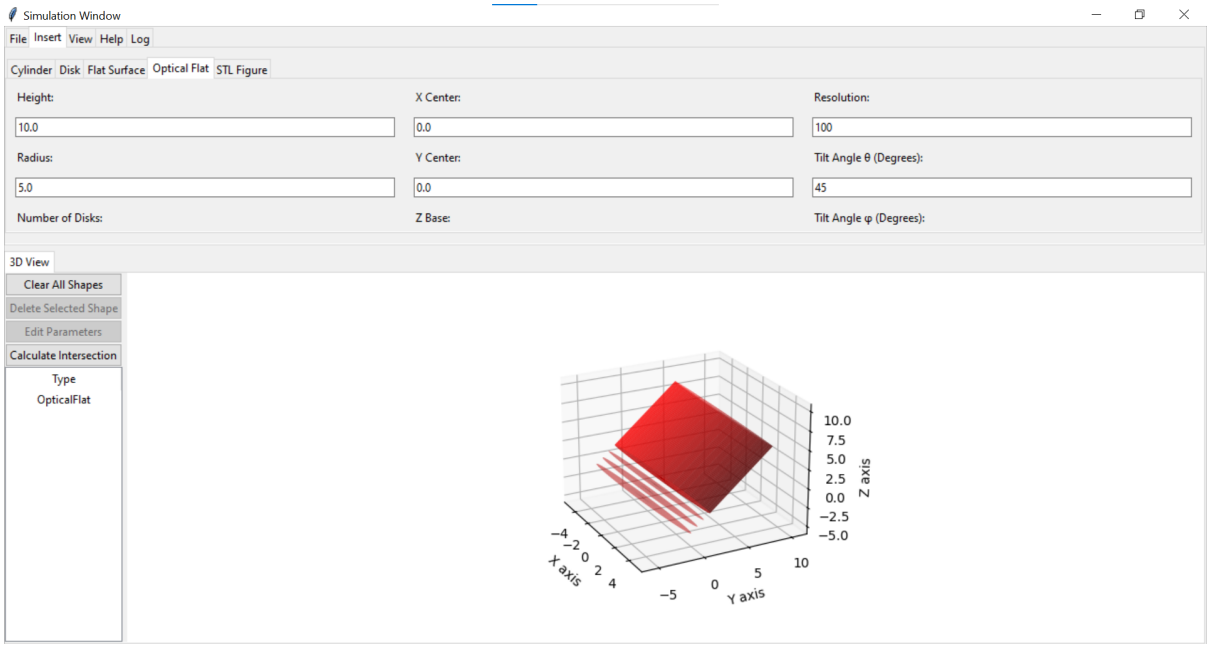


**Figure A.5.:** Configuration of an optical flat intersecting with multiple disks at an angle, highlighting the complex intersection capabilities of the tool.

### A.1.6. 3D Surface from Height Map Data

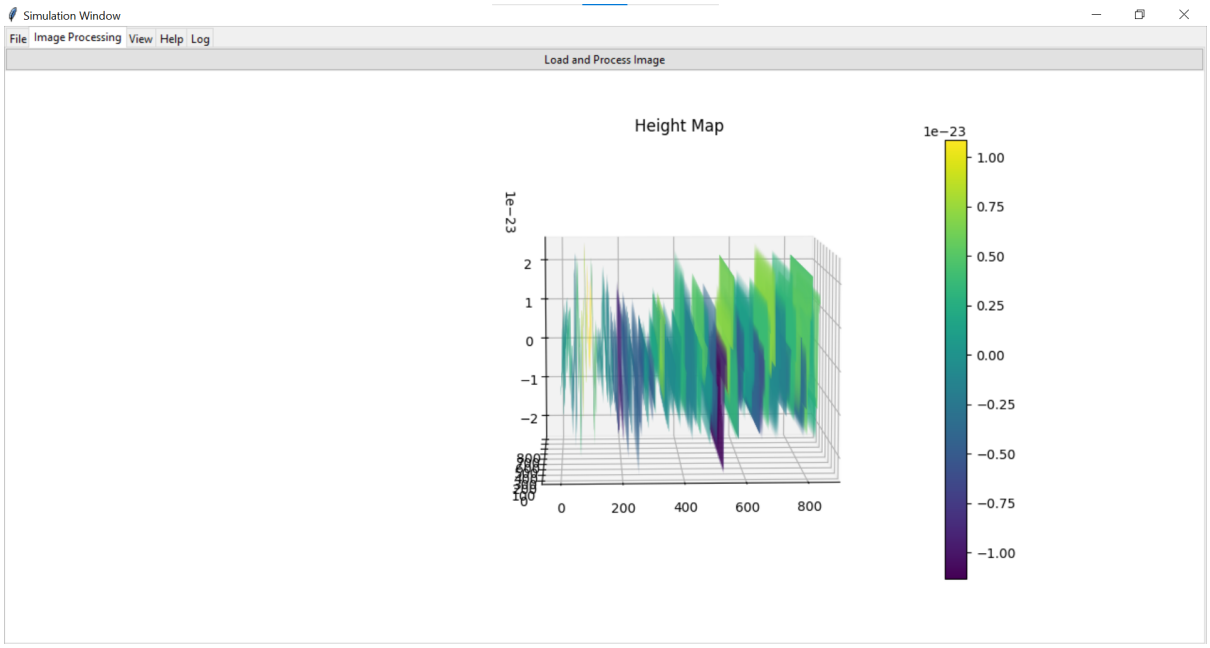


**Figure A.6.:** 3D visualization of a height map converted from image data, showing the application's ability to render surface topographies.

## A.1.7. Log File Output

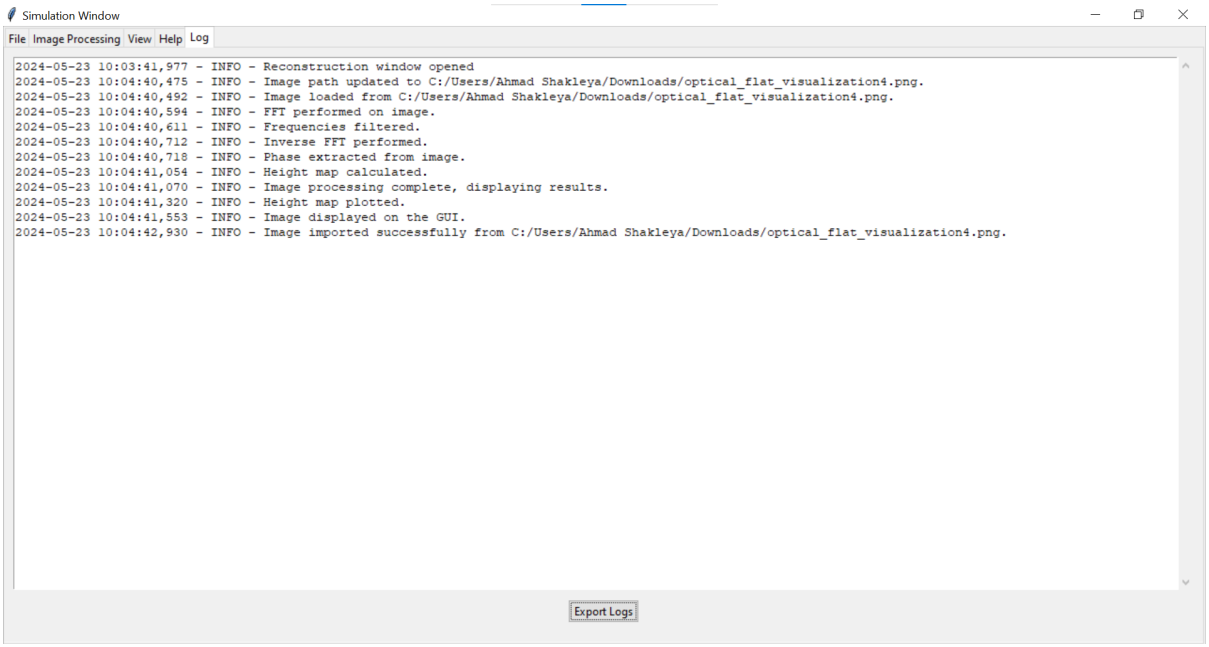


**Figure A.7.:** Log file output of the application capturing various steps such as loading images, processing FFT, and generating height maps.